

## BITWIST 3-MANIFOLDS

J.W. CANNON, W.J. FLOYD, AND W.R. PARRY

**Abstract.** Our earlier twisted-face-pairing construction showed how to modify an arbitrary orientation-reversing face-pairing on a faceted 3-ball in a mechanical way so that the quotient is automatically a closed, orientable 3-manifold. The modifications were, in fact, parametrized by a finite set of positive integers, arbitrarily chosen, one integer for each edge class of the original face-pairing. This allowed us to find very simple face-pairing descriptions of many, though presumably not all, 3-manifolds.

Here we show how to modify the construction to allow negative parameters, as well as positive parameters, in the twisted-face-pairing construction. We call the modified construction the *bitwist* construction. We prove that all closed connected orientable 3-manifolds are *bitwist* manifolds. As with the *twist* construction, we analyze and describe the Heegaard splitting naturally associated with a *bitwist* description of a manifold.

## 1. Introduction

In a series ([1, 2, 3]) of papers, we described and analyzed a simple construction of 3-manifolds from face-pairings. If  $\phi$  is an orientation-reversing edge-pairing on a polygonal disk  $D$ , then the quotient space  $D/\phi$  is always a surface. But if  $\phi$  is an orientation-reversing face-pairing on a faceted 3-ball  $P$ , the quotient  $P/\phi$  is not generally a 3-manifold. (See, for example, Section 2.7 of [4].) For the *twist* construction one chooses a positive integer, called the *multiplier*, for each edge cycle (equivalence class of an edge under the action of  $\phi$ ). By subdividing each edge into the product of its multiplier and the size of its edge cycle and then precomposing with a *twist*, one obtains a new faceted 3-ball  $Q$  and orientation-reversing face pairing  $\psi$ . The fundamental result of the construction is that  $Q/\psi$  is always a 3-manifold. Papers [1] and [2] give the basic details of the construction. The construction is analyzed further in [3], and Heegaard diagrams and surgery diagrams are given for twisted face-pairing manifolds.

In this paper we give a modified construction which we call the *bitwist* construction. The basic setup is the same, but we allow the edge cycle multipliers to be positive or negative. Allowing twisting in different directions leads to problems in defining the new face-pairing  $\psi$ , but one can resolve this by the appropriate insertion of "stickers" in the faces of the new faceted 3-ball  $Q$ . In Section 2 we give a simple preliminary example to show how stickers are used in the construction. Following this, we give the general construction in Section 3. As with the *twist* construction, the 3-manifolds constructed from the *bitwist* construction naturally have a cell structure with a single vertex. One can easily give presentations for

---

Date: February 20, 2024.

1991 Mathematics Subject Classification. 57Mxx.

Key words and phrases. 3-manifold constructions, surgeries on 3-manifolds, Thurston's geometries.

fundamental groups of bitwist manifolds as in [2, Section 4], but the homology results of [2, Section 6] do not generally hold for bitwist manifolds. Since  $Q =$  has a single vertex, some of the results from the twist construction apply directly to the bitwist construction. In particular, the construction of Heegaard diagrams and framed surgery descriptions from [3] are valid for the bitwist construction. This is developed in Section 4. If  $L$  is a corridor complex link for an orientation-reversing face pairing on a faceted 3-ball  $P$  and  $\text{mul}$  is a multiplier function for  $(P; )$ , then the bitwist manifold  $M(P; ; \text{mul})$  is obtained by framed surgery on  $L$ , where the face components have framing 0 and an edge component has framing the sum of its blackboard framing and the reciprocal of the multiplier of its edge cycle.

After making the leap to negative multipliers, it is natural to inquire about multipliers with value 0. Allowing edge cycle multipliers to be 0 amounts to collapsing every edge with multiplier 0 to a point and applying the construction to the resulting complex. In terms of our surgery description, this amounts to deleting from our framed link every component with framing 1, an operation which does not change the resulting manifold. Collapsing edges in general leads to complexes which are no longer 3-balls (they are cactoids). While we actually do find face-pairings on cactoids interesting and we do temporarily allow multipliers to be 0 in the proof of Theorem 5.5.1, for the present we content ourselves with nonzero multipliers.

The framed surgery descriptions are a primary motivation for developing the bitwist construction. In order to realize 3-manifolds as twisted face-pairing manifolds or bitwist manifolds, one wants to be able to change the framings of the edge components. Suppose  $L$  is a corridor complex link for a twisted face-pairing manifold. We still get a twisted face-pairing manifold if we replace the framing of each edge component by its blackboard framing plus an arbitrary positive rational number. In Section 5 we show that using the bitwist construction, we still get a bitwist manifold if we replace the framing of each edge component by its blackboard framing plus an arbitrary rational number. This ability to change the signs of the rational numbers gives extra power to the construction. Using this, we show in Section 6 that every closed connected orientable 3-manifold is a bitwist manifold.

## 2. A preliminary example

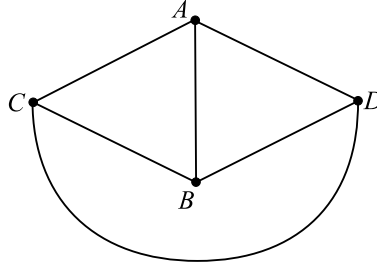
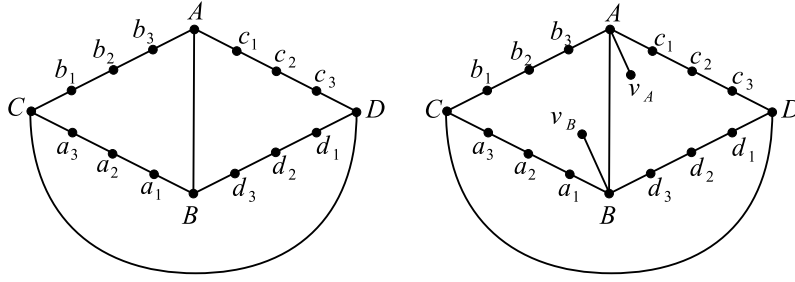
We give a preliminary example to indicate the construction. We start with a simple model face-pairing that was considered in Section 2 of [1]. Our faceted 3-ball  $P$  is a tetrahedron with vertices  $A, B, C$ , and  $D$ , as shown in Figure 1. We consider  $P$  as an oriented 3-ball, and for convenience give it an orientation so that in the induced orientation on the boundary of  $P$  the boundary of each 2-cell is oriented clockwise.

The model face pairing identifies the triangles  $ABC$  and  $ABD$  by reflection in the common edge  $AB$ , and it identifies  $ACD$  and  $BCD$  by reflection in the common edge  $CD$ . In the permutation notation of [1], is given as follows:

$$\begin{array}{l} 1 : \begin{array}{ccc} A & B & C \\ & A & B & D \end{array} \quad 2 : \begin{array}{ccc} A & C & D \\ & B & C & D \end{array} : \end{array}$$

There are three edge cycles, as follows:

$$\begin{array}{l} AB \xrightarrow{1} AB \\ BC \xrightarrow{1} BD \xrightarrow{2} AD \xrightarrow{1} AC \xrightarrow{2} BC \end{array}$$

Figure 1. The tetrahedron  $P$ .Figure 2. The subdivisions  $Q^0$  and  $Q$  of  $P$ .

$$CD \stackrel{?}{=} CD :$$

The first edge cycle  $[AB]$  has length  $\ell([AB]) = 1$ , the second edge cycle  $[BC]$  has length  $\ell([BC]) = 4$ , and the third edge cycle  $[CD]$  has length  $\ell([CD]) = 1$ . In the twisted face-pairing construction, for each edge cycle one chooses a positive integer  $\text{mul}([e])$  called the multiplier. For the bitwist construction, one chooses a nonzero integer  $\text{mul}([e])$ , still called the multiplier, for each edge cycle. We use the cycle lengths and the absolute values of the multipliers to determine how to subdivide the edges of  $P$ . The sign of the multiplier indicates the direction in which we twist edges in the edge cycle  $[e]$ . If all of the multipliers have the same sign, then we have the twist construction. For this example, we choose  $\text{mul}([AB]) = -1$ ,  $\text{mul}([BC]) = 1$ , and  $\text{mul}([CD]) = 1$ .

We are now ready to replace  $P$  by its subdivision  $Q$ . We subdivide every edge  $e$  of  $P$  into  $\ell([e]) \cdot |\text{mul}([e])|$  subedges. We perform these subdivisions so that the face-pairing takes subedges to subedges. Let  $Q^0$  be the resulting faceted 3-ball. We need to perform a further modification if the multipliers do not all have the same sign. Let  $f$  be a face of  $P$ . Suppose  $v$  is a vertex of  $P$  in  $f$ . Let  $e_1$  be the edge of  $P$  in  $f$  with terminal vertex  $v$  and let  $e_2$  be the edge of  $P$  in  $f$  with initial vertex  $v$ . If  $\text{mul}([e_1]) < 0$  and  $\text{mul}([e_2]) > 0$ , then we add a sticker (think straight pin with spherical head) to  $f$  at  $v$ . That is, we add a new vertex in the interior of  $f$  and join it to  $v$  by an edge in  $f$ . The faceted 3-ball obtained from  $P$  by adding stickers to  $Q^0$  as described above is the subdivision  $Q$ . Figure 2 shows the subdivisions  $Q^0$  and  $Q$  for this example.

We define a bitwisted face-pairing on  $Q$  as follows:

$$\begin{aligned} 1 : & \begin{array}{cccccccccccc} b_3 & A & B & v_B & B & a_1 & a_2 & a_3 & C & b_1 & b_2 \\ A & v_A & A & B & d_3 & d_2 & d_1 & D & c_3 & c_2 & c_1 \end{array} ; \\ 2 : & \begin{array}{cccccccc} c_1 & A & b_3 & b_2 & b_1 & C & D & c_3 & c_2 \\ B & a_1 & a_2 & a_3 & C & D & d_1 & d_2 & d_3 \end{array} : \end{aligned}$$

The underlying idea is that we precompose with a twist in the positive direction on an edge which is a subedge of an original edge with positive multiplier, and we precompose with a twist in the negative direction on an edge which is a subedge of an original edge with negative multiplier. This is not well defined on  $Q^0$  since adjacent original edges can have multipliers of different signs, but one can make it well defined on  $Q$ .

Let  $M = Q =$ , where is the equivalence relation on  $Q$  generated by the face-pairing. The computation below shows that  $M$  has two 1-cells and a single 0-cell.

$$\begin{aligned} b_3 A & \stackrel{1}{\sim} A v_A \stackrel{1}{\sim} B A \stackrel{1}{\sim} v_B B \stackrel{1}{\sim} B d_3 \stackrel{2}{\sim} c_1 c_2 \stackrel{1}{\sim} b_2 b_1 \stackrel{1}{\sim} \\ & a_3 C \stackrel{1}{\sim} D c_3 \stackrel{1}{\sim} d_1 d_2 \stackrel{1}{\sim} a_2 a_1 \stackrel{2}{\sim} b_3 A \\ b_1 C & \stackrel{1}{\sim} C D \stackrel{1}{\sim} D d_1 \stackrel{1}{\sim} a_3 a_2 \stackrel{2}{\sim} b_2 b_3 \stackrel{1}{\sim} \\ & c_1 A \stackrel{1}{\sim} B a_1 \stackrel{1}{\sim} d_3 d_2 \stackrel{2}{\sim} c_2 c_3 \stackrel{1}{\sim} b_1 C \end{aligned}$$

Since  $M$  has two 2-cells and a single 3-cell,  $(M) = 0$  and so  $M$  is a 3-manifold. Figure 3 shows the link of the vertex of  $M$ . As for the twist construction,  $M$  can also be obtained as the quotient under the face pairings of a dual faceted 3-ball  $@Q$ , and the boundary of  $@Q$  is cellularly isomorphic to the dual of the link shown in Figure 3. The subdivision of  $@Q$  is shown in Figure 4. It is easy to see from Figure 4 or from the display above that

$$\begin{aligned} 1(M) &= hx; y: xx^1 x^1 xy^1 x^1 yxyx^1 y^1; yxyx^1 y^1 xyxy^1 x^1 i \\ &= hx; y: y^2 x^1 yxyx^1; y^2 x^1 y^1 xyxy^1 x^1 i: \end{aligned}$$

### 3. The bitwist construction

We now give the main construction. In [2] we defined a faceted 3-ball to be a regular CW complex. Here we follow the more general definition of a faceted 3-ball  $P$  given in [3]. In particular, we do not assume that the 2-cells in  $@P$  are regular. As in [3], a faceted 3-ball  $P$  is an oriented CW complex such that  $P$  is a closed 3-ball, there is a single 3-cell and its interior is  $\text{int}(P)$ , and  $@P$  does not consist solely of a 0-cell and a 2-cell. It follows from this that for each 2-cell  $f$  of  $P$ , there is a CW structure on a closed disk  $F_f$  such that i)  $F_f$  has a single 2-cell and its interior is  $\text{int}(F_f)$  and ii) there is a continuous cellular map  $f' : F_f \rightarrow f$  whose restriction to each open cell is a homeomorphism.

Still following [3], given a faceted 3-ball  $P$  we construct a subdivision  $P_s$  of  $P$  by barycentrically subdividing  $@P$ . The faceted 3-ball  $P_s$  is a regular CW complex and each 2-cell of  $P_s$  is a triangle. Since the 2-cells of  $P$  may not be regular, a face pairing on  $P$  is technically a matching of the faces of  $P$  together with a face

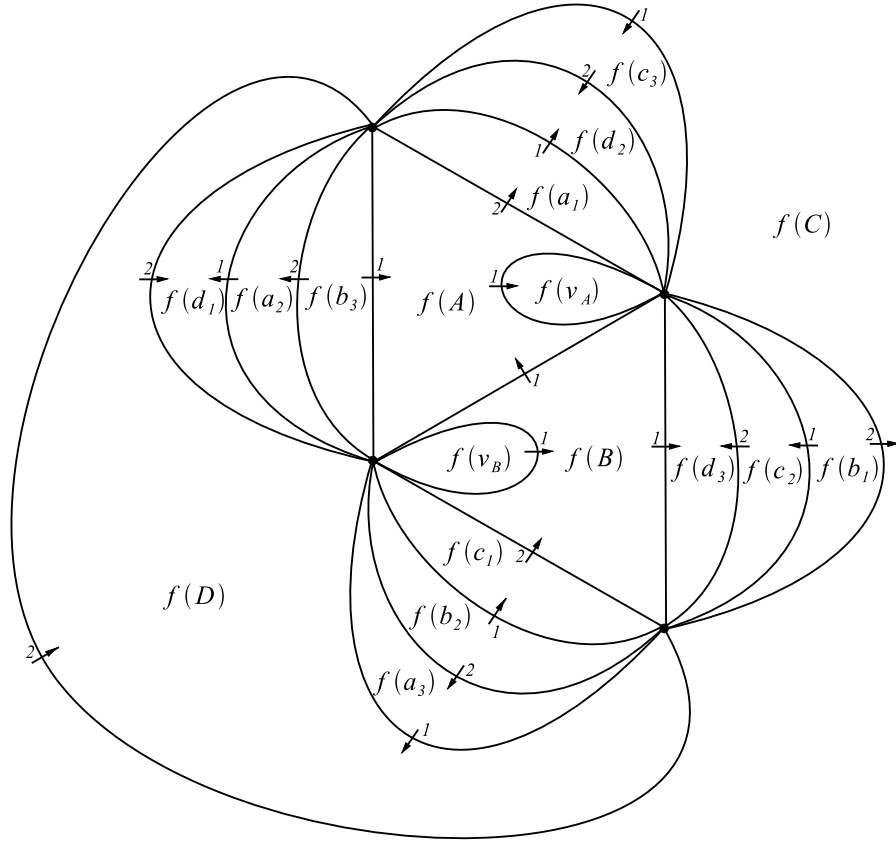
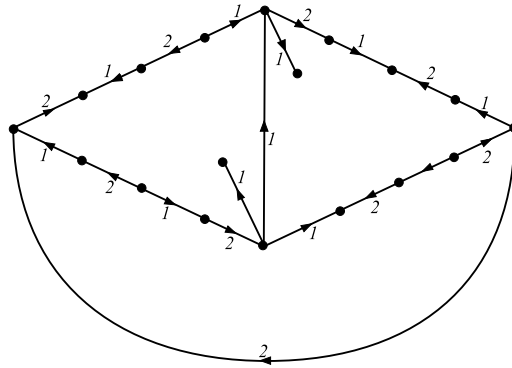
Figure 3. The link of the vertex of  $M$ .

Figure 4. The dual subdivision.

pairing on  $P_s$  which is compatible with it. We still denote by  $\phi$  the face pairing on  $P_s$ . We assume as before that our face-pairings reverse orientation and satisfy the face-pairing compatibility condition.

Suppose  $P$  is a faceted 3-ball and  $\sim$  is a face-pairing on  $P$ . We refer to  $\sim$  as a model face-pairing. There is an equivalence relation  $\sim$  defined on the edges of  $P$  that is generated by the relation  $e_1 \sim e_2$  if  $e_2$  is the image of  $e_1$  under some element of  $\sim$ ; the equivalence classes are called edge cycles. If  $[e]$  is an edge cycle, we denote its cardinality by  $\ell([e])$  and call it the length of  $[e]$ . In addition to  $(P; \sim)$ , the input for the bitwisted construction consists of a multiplier function. The multiplier function is a function  $\text{mul}: \text{edge cycles} \rightarrow \mathbb{Z} \setminus \{0\}$ . An edge  $e$  is positive if  $\text{mul}([e]) > 0$  and is negative if  $\text{mul}([e]) < 0$ .

Suppose we are given a face-pairing  $(P; \sim)$  together with a multiplier function  $\text{mul}$ . We create a subdivision  $Q$  of  $P$  in two stages. The first stage consists of subdividing each edge  $e$  of  $P$  into  $\ell([e]) \cdot \text{mul}([e])$  subedges to get a subdivision  $Q^0$  of  $P$ , and forming the subdivision  $Q_s^0$  of  $Q^0$  by barycentrically subdividing  $\partial Q^0$ . We perform these subdivisions so that  $\sim$  defines a face-pairing  $\sim^0$  on  $Q_s^0$ . The second stage of our construction of  $Q$  consists of adding stickers at some of the corners of the faces of  $Q^0$ . Suppose  $f$  is a face of  $P$ , and consider a corner of  $f$  at a vertex  $v$  with edges  $e$  and  $e^0$ , labeled such that  $e^0$  precedes  $e$ . Suppose that  $e^0$  is a negative edge and  $e$  is a positive edge. Let  $a$  be the edge of  $Q_s^0$  which bisects this corner. To  $Q^0$  we add a barycenter  $u$  of  $a$  and the subedge of  $a$  joining  $u$  and  $v$ . This subedge of  $a$  is a sticker. We continue with this process for all of the corners of all of the faces of  $P$ . The result is a faceted 3-ball  $Q$  which is obtained from  $P$  by subdividing edges and adding stickers.

As for  $P$  and  $Q^0$ , we form the subdivision  $Q_s$  from  $Q$  by barycentrically subdividing  $\partial Q$ . We do this so that  $Q_s$  is a subdivision of  $Q_s^0$ . If  $f$  is a face of  $P$ , we will still use the name  $f$  for the corresponding face in  $Q$ ; to cut down on the confusion, we will refer to edges of  $P$  in  $f$  as original edges and to vertices of  $P$  in  $f$  as original vertices. Note that  $Q_s$  can be obtained from  $Q_s^0$  by splitting certain edges which connect original vertices to barycenters of faces and then for each split edge inserting a digon decomposed into four triangles. See Figure 5, where the edge of  $Q$  joining  $u$  and  $v$  is a sticker. In particular, there is a correspondence between faces of  $Q_s^0$  and faces of  $Q_s$  that do not contain subedges of stickers.

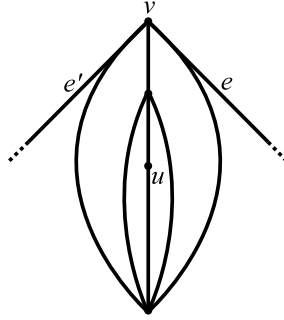


Figure 5. The subdivision of a face of  $Q_s$  near a sticker.

We next define a bitwisted face-pairing  $\sim$  on  $Q_s$ . The orientation on  $P$ , and hence on  $Q$  and  $Q_s$ , determines a cyclic order on the boundary of each face  $f$  of  $Q$  and hence a cyclic order on the faces of the subdivision  $f_s$ .

Let  $f$  be a face of  $Q$ , and let  $e$  be an edge of  $f_s$  which is part of an originaledge  $a$  of  $P$ . See Figure 6, which shows part of  $f_s$  and  $f_s^{-1}$  for some face  $f$  of  $Q$  with positive originaledge  $a$ . The vertices and edges of  $f$  and  $f^{-1}$  are drawn thick for emphasis. Let  $t$  be a face of the subdivision  $f_s$  which contains  $e$ . If  $a$  is a positive edge, let  $\varepsilon(t)$  be the face of  $f_s^{-1}$  which is the second face before the face  $\delta(t)$  of  $f_s^{-1}$ . If  $a$  is a negative edge, let  $\varepsilon(t)$  be the face of  $f_s^{-1}$  which is the second face after the face  $\delta(t)$  of  $f_s^{-1}$ . Figure 7 shows  $\varepsilon(t)$  and  $\delta(t)$  for certain faces  $t_1$  and  $t_2$  of  $f_s$  for the case in which  $f$  has a sticker. The faces  $t_1$  and  $t_2$  both contain an original vertex which is contained in the sticker. Note that in  $f_s^{-1}$  from  $\varepsilon(t)$  to  $\delta(t)$  in the positive direction there are four faces corresponding to the four faces of  $f_s$  which contain a subedge of the sticker. It follows that the definition of  $\varepsilon$  can be extended to a face-pairing between  $f_s$  and  $f_s^{-1}$ . Doing this for each face defines a face-pairing on  $Q$ . Unless the sign of  $\text{mul}$  is constant, this will not define a face-pairing on  $Q^0$ . In effect we are using the sign of  $\text{mul}$  to determine which direction to twist each face of  $Q_s$ ; the stickers enable us to make this well defined.

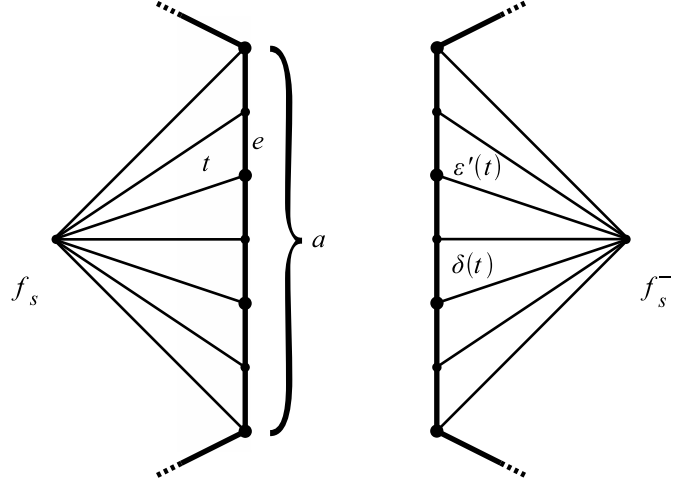


Figure 6. Defining the bitwisted face-pairing  $\varepsilon$ .

We denote by  $M(P; \varepsilon; \text{mul})$  the quotient space of  $Q$  under the equivalence relation generated by  $\varepsilon$ .

**Theorem 3.1.** Let  $P$  be a faceted 3-ball, let  $\varepsilon$  be an orientation-reversing face-pairing on  $P$  and let  $\text{mul}$  be a multiplier function for  $(P; \varepsilon)$ . Then  $M = M(P; \varepsilon; \text{mul})$  is a closed 3-manifold. Furthermore, as a cell complex  $M$  has just one vertex.

*Proof.* The proof of the first assertion is an Euler-characteristic argument analogous to the argument in [1]. To prove that  $M$  is a closed 3-manifold, it suffices to show that  $\chi(M) = 0$ . We do this by determining the number of cells in  $M$  of every dimension. It is clear that  $M$  has one 3-cell and that the number of 2-cells is the number of pairs of faces of  $Q$ . So to prove Theorem 3.1, it suffices to prove that  $M$  has one 0-cell and that the number of 1-cells is the number of pairs of faces of  $Q$ .

Every edge of  $Q$  is either a sticker or a subedge of an originaledge. The discussion involving Figure 7 shows that the image under  $\varepsilon$  of a sticker contained in a face  $f$  of

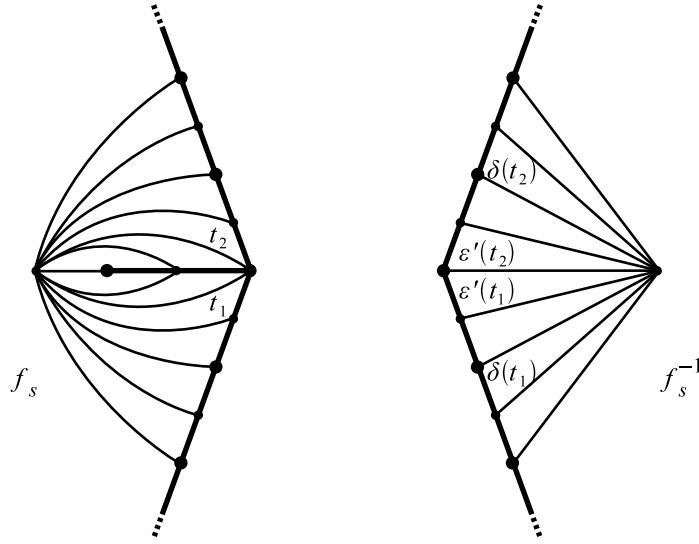


Figure 7. Defining a sticker.

$Q$  consists of two edges of  $f^{-1}$ . One of these edges of  $f^{-1}$  is a terminal subedge of a positive original edge and one is an initial subedge of a negative original edge. The discussion involving Figure 6 implies that every edge of  $Q$  contained in an original edge is equivalent to an edge  $e$  of a face  $f$  of  $Q$  such that either  $e$  is the terminal subedge of a positive original edge of  $f$  or  $e$  is the initial subedge of a negative original edge of  $f$ . We conclude that every edge of  $Q$  is equivalent to an edge  $e$  of a face  $f$  such that either  $e$  is the terminal subedge of a positive original edge of  $f$  or  $e$  is the initial subedge of a negative original edge of  $f$ . Also, if  $f$  is a face of  $Q$  with a positive original edge  $e$  followed immediately by a negative original edge  $e^0$ , then the terminal subedge of  $e$  is equivalent to the initial subedge of  $e^0$  by means of a sticker. Moreover every vertex of  $Q$  is equivalent to an original vertex.

Now let  $e_0$  be an edge of a face  $f_0$  of  $Q$  such that  $e_0$  is the terminal subedge of a positive original edge of  $f_0$ . Also suppose that the original edge of  $f_0$  immediately following  $e_0$  is positive. By considering the  $\sigma$ -orbit of  $e_0$  we obtain edges  $e_1; \dots; e_n$  of faces  $f_1; \dots; f_n$  of  $Q$  and original edges  $e_1^0; \dots; e_n^0$  with the following properties.

$$\begin{aligned} n &= \text{card}(\{e_i^0\}) \text{ in } \text{ul}(\{e_i^0\}) \text{ for } i \geq 1; \dots; n \\ e_i^0 &= f_i \setminus f_{i-1}^{-1} \text{ for } i \geq 1; \dots; n \\ e_i &\text{ is the } i\text{th subedge of } e_i^0 \text{ relative to } f_i \text{ for } i \geq 1; \dots; n \end{aligned}$$

We see that  $f_n = f_0$ , that  $e_n^0$  is the original edge of  $f_0$  immediately following  $e_0$ , that  $e_n$  is the terminal subedge of  $e_n^0$  relative to  $f_0$ , that  $e_0$  and  $e_n$  are equivalent in an orientation-preserving way, that  $e_1$  is the terminal subedge of a positive original edge of  $f_0^{-1}$  and that none of the edges  $e_2; \dots; e_{n-1}$  is the terminal subedge of an original edge relative to either face containing it. Corresponding statements hold if  $e_0$  is an initial subedge of a negative original edge of  $f_0$ .

The previous paragraph implies for every face  $f$  of  $Q$  that the terminal subedges of positive original edges of  $f$  and  $f^{-1}$  and the initial subedges of negative original



edges of  $f$  and  $f^{-1}$  are allequivalent and they are not equivalent to any other such edges of other faces. This and the results of the next-to-last paragraph establish a bijection between the 1-cells of  $M$  and pairs of faces of  $Q$ . Similarly, the last paragraph implies for every face of  $Q$  that its original vertices are equivalent. This and the results of the next-to-last paragraph imply that  $M$  has just one 0-cell.

This proves Theorem 3.1.

We denote by  $Q$  the subdivision of  $P$  obtained by replacing the multiplier function  $\text{mul}$  by  $\text{mul}$ .

Theorem 3.2. Let  $P$  be a faceted 3-ball, let  $\epsilon$  be an orientation-reversing face-pairing on  $P$ , and let  $\text{mul}$  be a multiplier function for  $(P; \epsilon)$ . Then the dual of the link of the vertex of  $M$  is isomorphic to  $@Q$  in an orientation-reversing way.

Proof. The proof is an adaptation of the arguments for the analogous results in [2] and [3]. Suppose  $f$  is a face of  $P$  and  $e$  is an edge of  $P$  in  $f$ . First suppose that  $e$  is a positive edge. Let  $a$  be the initial vertex of  $e$  relative to  $f$ , let  $b$  be the terminal vertex of  $e$  relative to  $f$ , and let  $h$  be the edge of  $Q$  preceding  $e$  in  $f$ . Let  $x$  be the vertex of  $M$ . The image of  $\text{link}(a; Q)$  in  $\text{link}(x; M)$  has a vertex corresponding to  $h$ , and this vertex is in a chain of  $\text{mul}(e) + 1$  faces; the first face is the image of  $\text{link}(a; Q)$ , the last face is the image of  $\text{link}(b; Q)$  and all of the other faces are digons which are the images of links of vertices of  $Q$  that are not vertices of  $P$ . Similarly, if  $e$  is a negative edge,  $a$  is the terminal vertex of  $e$  relative to  $f$ ,  $b$  is the initial vertex of  $e$  relative to  $f$ , and  $h$  is the edge of  $Q$  following  $e$  in  $f$ , then the vertex corresponding to  $h$  in the image of  $\text{link}(a; Q)$  in  $\text{link}(x; M)$  is in a chain of  $\text{mul}(e) + 1$  faces joining the images of  $\text{link}(a; Q)$  and  $\text{link}(b; Q)$ . So in each case, in the dual of  $\text{link}(x; M)$  there is a segment subdivided into  $\text{mul}(e)$  edges which joins the duals of the images of  $\text{link}(a; Q)$  and  $\text{link}(b; Q)$ .

We next need to see how these segments fit together. We suppose for convenience that  $e$  is a positive edge. Let  $e^0$  be the edge of  $P$  that precedes  $e$  in  $f$  and let  $e^0$  be the edge of  $P$  that follows  $e$  in  $f$ . If  $e^0$  is also a positive edge, then in the dual of  $\text{link}(x; M)$  there is a face containing a pair of adjacent segments, subdivided into  $\text{mul}(e)$  and  $\text{mul}(e^0)$  edges. A similar statement holds if  $e^0$  is a positive edge. If  $e^0$  is a negative edge, then the edge of  $Q$  preceding  $e$  in  $f$  is a sticker, and is the same as the edge of  $Q$  following  $e^0$  in  $f$ . This sticker is the edge  $h$  of the previous paragraph for both  $e$  and  $e^0$ . So in the dual of  $\text{link}(x; M)$  the segments corresponding to  $e$  and  $e^0$  are adjacent in some face. If  $e^0$  is a negative edge, then the terminal subedge of  $e$  in  $f$  and the initial subedge of  $e^0$  in  $f$  are equivalent to a sticker in the face  $f^{-1}$ , and so there is a sticker in the dual of  $\text{link}(x; M)$  between the segments corresponding to  $e$  and  $e^0$ . A similar analysis holds if  $e$  is a negative edge.

This implies that in the dual of  $\text{link}(x; M)$  there is a face corresponding to  $f$  that is cellularly homeomorphic to the face corresponding to  $f$  in  $Q$ . This correspondence between faces of  $Q$  and faces of the dual of  $\text{link}(x; M)$  respects adjacency of faces. So the dual of  $\text{link}(x; M)$  is cellularly homeomorphic to  $@Q$ . It follows as in [2] that this homeomorphism reverses orientation.

Remark 3.3. The proof of Theorem 3.2 interpreted in terms of dual cap subdivision shows just as in [2] and [3] that the manifolds  $M(P; \text{mul})$  and  $M(P; \text{mul})$  are

homeomorphic by means of a map which establishes a duality between these cell complexes.

#### 4. Heegaard diagrams for bitwist manifolds

Let  $M = M(P; \mu)$  be a bitwist manifold, let  $Q$  be the corresponding subdivision of  $P$ , and let  $\phi$  be the corresponding bitwisted face-pairing on  $Q$ . As in [3, Section 4], one can construct the edge pairing surface  $S$  of  $(Q; \phi)$ . For each face  $f$  in  $Q$ , there is a CW structure on a closed disk  $F_f$  such that i)  $F_f$  has a single 2-cell whose interior is the interior of  $F_f$ , ii) there is a continuous cellular map  $\rho_f : F_f \rightarrow f$  whose restriction to each open cell in  $F_f$  is a homeomorphism, and iii) there is a continuous cellular map  $\sigma_f : F_f \rightarrow f^{-1}$  whose restriction to each open cell is a homeomorphism. (And also  $\rho_f$  and  $\sigma_f$  are compatible with respect to the face-pairing.) Let  $Y$  be the quotient of the union of the 1-skeleton  $X$  of  $Q$  and the finite union of the complexes  $\partial F_f \times [0; 1]$ , one for each pair  $(f; f^{-1})$ , under the equivalence relation generated by the identifications of  $(x; 0)$  with  $\rho_f(x)$  and  $(x; 1)$  with  $\sigma_f(x)$  for  $x \in \partial F_f$ . Then  $Y$  is an orientable closed surface, and the dual cap subdivision of  $Y$  is the edge pairing surface  $S$ . (See [3, Section 3] for the definition of the dual cap subdivision. The dual cap subdivision of a 2-complex is obtained from its barycentric subdivision by removing the edges joining vertices to barycenters of faces.) Edges of  $S$  that are contained in  $X$  or disjoint from  $X$  are called vertical, and the other edges of  $S$  are called diagonal. Edges of  $S$  that are not contained in edges of  $Y$  are called meridian edges, and edges of  $S$  contained in edges of  $Y$  are called nonmeridian edges.

**Theorem 4.1.** Let  $M = M(P; \mu)$  be a bitwist manifold, and let  $S$  be the edge pairing surface for the associated bitwisted face pairing. The union  $V$  of the vertical meridian edges is a basis of meridian curves for  $S$ , and the union  $D$  of the diagonal meridian edges is a basis of meridian curves for  $S$ . Furthermore  $(S; V; D)$  is a Heegaard diagram for  $M$ .

*Proof.* Since  $M = Q/\phi$  is a manifold with a single vertex, this follows immediately from [3, Theorem 4.2.1].

Figure 8 shows the union of  $\partial F_{f_1} \times [0; 1]$  and  $\partial F_{f_2} \times [0; 1]$  for the example from Section 2, where  $f_1$  is the triangle  $ABC$ ,  $f_2$  is the triangle  $ACD$ , and the two sides of the stickers have been identified.

As in [3], the surface  $S$  can also be decomposed into edge cycle cylinders. The only difference from the construction in [3] is that if  $f$  is a face of  $P$  and  $e$  is either a positive original edge which is preceded by a sticker or a negative original edge that is followed by a sticker, then the sticker is included with that edge in the construction of the edge cycle cylinder. For example, Figure 9 shows, for the example from Section 2, the edge cycle cylinders. Figure 10 shows, for the same example, the edge cycle cylinders with the stickers pushed back to be horizontal edges. Note that, in this view, vertical meridian edges are drawn vertically and diagonal meridian edges are drawn diagonally. This view makes the effect of adding the stickers more apparent. When a diagonal meridian edge crosses a sticker, it changes direction. This reflects the difference in directions of twists corresponding to edge cycles with positive multipliers and edge cycles with negative multipliers.

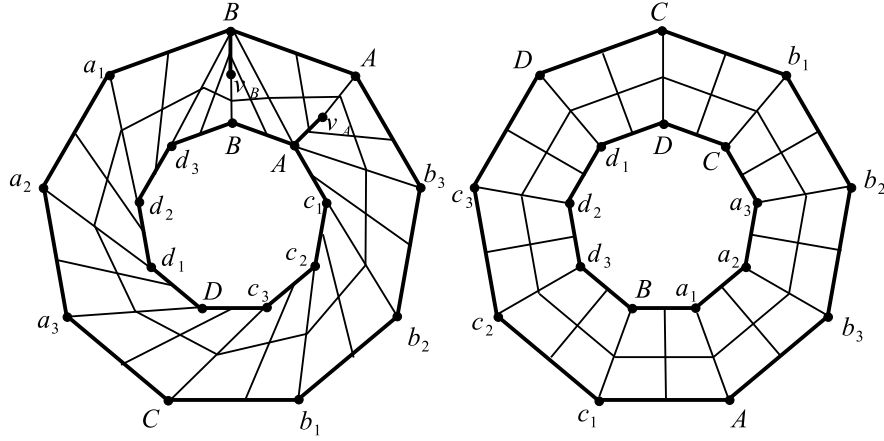
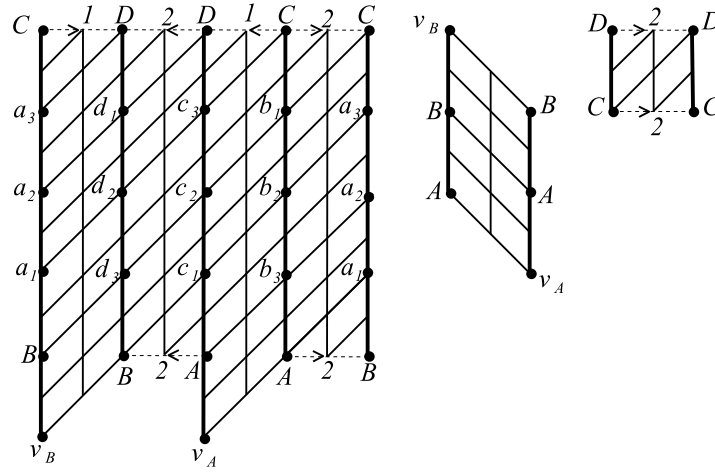
Figure 8.  $@F_{f_1} [0;1]$  and  $@F_{f_2} [0;1]$  for the example from Section 2.

Figure 9. The edge cycle cylinders for the example from Section 2.

Let  $C$  be an edge cycle cylinder, where as in Figure 10 we have pushed the stickers back to be horizontal. Let  $\mathcal{C}^0$  be a minimal union of vertical (resp. diagonal) meridian edges that joins the two horizontal ends of  $C$ , chosen so that  $@ = @^0$ . Let  $\mathcal{C}$  be a simple closed curve in  $C$  that separates the ends of  $C$ , and let  $m = \text{mul}(\mathcal{C})$ , where  $\mathcal{C}$  is the edge cycle associated to  $C$ . Then  $\mathcal{C}^0$  is isotopic rel endpoints to  $\mathcal{C}^m$ , where  $\mathcal{C}^m$  is a Dehn twist along  $\mathcal{C}$ . Furthermore, as one repeats this construction for the other edge cycle cylinders, the directions of the Dehn twists can all be chosen consistently with respect to an orientation of  $S$ .

**Theorem 4.2.** Let  $M = M(P; \text{mul})$  be a bitwist manifold, let  $S$  be the edge pairing surface for the associated bitwisted face pairing, and let  $V = f_1; \dots; f_n$  be the vertical meridian curves as in Theorem 4.1. Let  $E_1; \dots; E_m$  be the edge cycles of  $S$ . For each  $i \in \{1, \dots, m\}$  let  $C_i$  be the edge cycle cylinder associated to  $E_i$  and let  $\mathcal{C}_i$  be a Dehn twist along a simple closed curve in  $C_i$  which separates the ends of  $C_i$ .

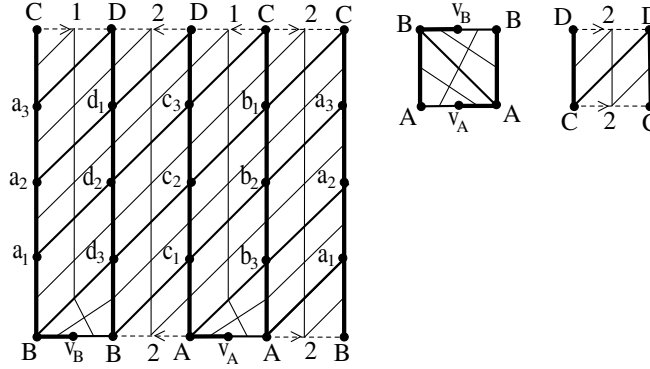


Figure 10. Another view of the edge cycle cylinders for the example from Section 2.

We choose the  $\alpha_i$ 's so that they twist in consistent directions with respect to a fixed orientation of  $S$ . Let  $\mu = \frac{\text{mul}(E_1)}{1} \dots \frac{\text{mul}(E_m)}{m}$ . Then  $(S; V; f(\alpha_1); \dots; (\alpha_n)g)$  is a Heegaard diagram for  $M$ .

Proof. This follows immediately from Theorem 4.1 and the discussion in the paragraph before the statement of the theorem.

The construction of corridor complex links for bitwist 3-manifolds is the same as their construction in [3, Section 6] for twisted face-pairing manifolds, though the framings change because of the signs of the multipliers. We first recall the construction of corridor complex links.

Suppose  $P$  is a faceted 3-ball,  $\alpha$  is an orientation-reversing face-pairing on  $P$ , and  $\text{mul}$  is a multiplier function for  $\alpha$ . Let  $M = M(P; \alpha; \text{mul})$  be the associated bitwist 3-manifold. We form a corridor complex for  $M$  as follows. We choose a pair  $f_1$  and  $f_2$  of faces in  $\partial P$  that are matched by  $\alpha$ , and choose an edge-path arc in the 1-skeleton of  $\partial P$  that joins a corner of  $f_1$  to its image under  $\alpha$  in  $f_2$ . We then split this edge-path to a thin corridor. This gives a new cell structure on  $\partial P$  in which the old faces  $f_1$  and  $f_2$  have been joined by the corridor into a single face. We do this successively for all of the face pairs of  $\partial P$ , and call the resulting cell structure on  $\partial P$  the corridor complex  $C$ .

We next describe a link  $L$  in  $S^3$  in terms of its projection to  $C$ . For each face of  $C$  there is an unknotted component of  $L$  that lies in one of the old faces that are part of that face; we call this component a face component. Next consider one of the old faces  $f$  that contains a face component. Each edge of that old face corresponds to an edge of the corresponding face in the corridor complex. For each such edge  $e$ ,  $L$  contains an arc which enters the old face from the barycenter of the edge, crosses under the face component in the old face, crosses over the face component, goes through the corridor, and ends at the barycenter of the edge  $\alpha_f(e)$ . These arcs are constructed so that they have no self-crossings or intersections with other such arcs from that face. We construct these arcs for each face of the corridor complex. Suppose  $e$  is one of the original edges in  $P$ . If  $e$  has not been split in the construction of the corridor complex, then at the barycenter of  $e$  we have the ends of the arcs from the two faces that contain  $e$  (or from the face that meets  $e$  with

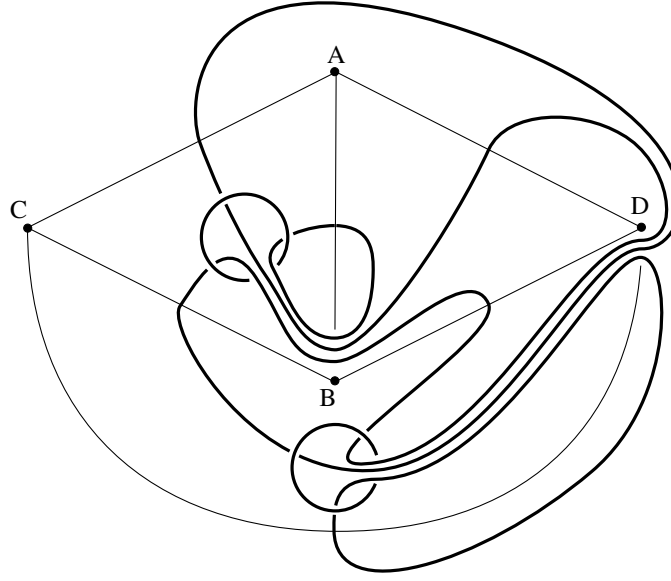


Figure 11. A corridor complex link for the example from Section 2.

multiplicity two). If  $e$  has been split in the construction of the corridor complex, then we join the ends of the two corresponding arcs by an arc that goes under the arcs in the corridor. The union of all of these arcs is a finite set of components of  $L$  that are called edge components. Each edge component crosses exactly those edges of  $C$  which correspond to an edge cycle of  $\mathcal{P}$ . The corridor complex link  $L$  is the union of the face components and the edge components. We call  $L$  a corridor complex link for  $(P; \mu)$ . A corridor complex link for the example from Section 2 is shown in Figure 11.

**Theorem 4.3.** Let  $M = M(P; \mu; \text{mul})$  be a bitwist 3-manifold, and let  $L$  be the corresponding corridor complex link. Define a framing on  $L$  by giving each face component framing 0 and giving the edge component corresponding to an edge cycle  $E$  the framing  $\text{mul}(E) - 1$  plus the blackboard framing of the edge component. Then Dehn surgery on the framed link  $L$  yields  $M$ .

**Proof.** This follows easily from the proofs of [3, Theorem 6.2.2] and [3, Theorem 6.1.2]. The proof of [3, Theorem 6.2.2] goes through in this greater generality until the last paragraph, when it refers to [3, Theorem 6.1.2]. The statement and proof of [3, Theorem 6.1.2] go through in this greater generality.

## 5. Generalizing framings of corridor complex links

In this section we develop some of the machinery needed for the proof of Theorem 6.2. We first discuss some well-known techniques for changing framed surgery descriptions of 3-manifolds. We then show that, in a sense made precise in Theorem 5.2.1, connected sums of corridor complex links are corridor complex links. Theorem 5.3.1, that connected sums of bitwist manifolds are bitwist manifolds, follows easily. We next consider a special family of face-pairings called reflection

face-pairings, and use them to show that every lens space is a twisted face-pairing 3-manifold. This allows us to prove Theorem 5.6.1, which states that if  $L$  is a complex corridor link, then for any choices of framings for the edge components we still get a twisted manifold by framed surgery.

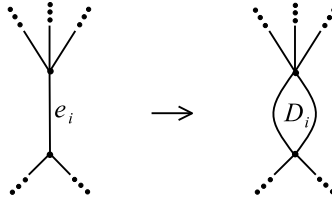
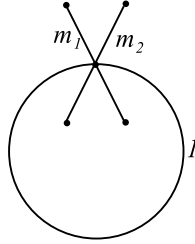
5.1. Dehn surgery preliminaries. We collect some well-known facts about Dehn surgery which will be used later.

We first discuss Rolfsen twists. They appear on page 162 of [5], they appear in Sections 16.4, 16.5 and 19.4 of [7] as Fenn-Rourke moves, and they appear in Section 9.H of [8]. For this let  $L$  be a link in  $S^3$  framed by the elements of  $Q$  [f.l.g.]. Let  $J$  be an unknotted component of  $L$ . Then  $L \setminus J$  is contained in a closed solid torus  $T$ , which is the complement in  $S^3$  of a regular neighborhood of  $J$ . Let  $\theta$  be a right hand Dehn twist of  $T$ . Let  $n \in \mathbb{Z}$ . Let  $L^0$  be the link gotten from  $L$  by applying  $\theta^n$  to  $L \setminus J$ . We frame  $L^0$  as follows. If the  $L$ -framing of  $J$  is  $r$ , then the  $L^0$ -framing of  $J$  is  $\frac{1}{n + \frac{1}{r}}$ . If  $K$  is a component of  $L$  other than  $J$  with framing  $r$ , then the image of  $K$  in  $L^0$  has framing  $r + n \cdot \text{lk}(J; K)$ , where  $\text{lk}(J; K)$  is the linking number of  $J$  and  $K$  after orienting  $J$  and  $K$  arbitrarily. When  $n = 1$ , we say that  $L^0$  is obtained from  $L$  by performing a Rolfsen twist about  $J$ . In general we obtain  $L^0$  by performing  $n$  Rolfsen twists about  $J$ . We are interested in Rolfsen twists because the manifold obtained by Dehn surgery on  $L^0$  is homeomorphic to the manifold obtained by Dehn surgery on  $L$ .

We next discuss slam-dunks. These appear on page 163 of [5]. Let  $L$  be a framed link in  $S^3$ . Suppose that one component  $K$  of  $L$  is a meridian of another component  $J$  and that  $K$  is contained in a topological ball in  $S^3$  which meets no components of  $L$  other than  $J$  and  $K$ . Suppose that the framing of  $J$  is  $n \in \mathbb{Z}$  and that the framing of  $K$  is  $r \in \mathbb{Q}$  [f.l.g.]. Let  $L^0$  be the framed link obtained from  $L$  by deleting  $K$  and changing the framing of  $J$  to  $n - \frac{1}{r}$ . We say that  $L^0$  is obtained from  $L$  by performing the slam-dunk which removes  $K$ . The manifold obtained by Dehn surgery on  $L^0$  is homeomorphic to the manifold obtained by Dehn surgery on  $L$ .

5.2. Connected sums of corridor complex links. Here we establish the fact that the links obtained from the corridor construction are closed under the operation of connected sum in a certain restricted sense.

We begin with two faceted 3-balls  $P_1$  and  $P_2$ . For  $i \in \{1, 2\}$  let  $\alpha_i$  be an orientation-reversing face-pairing on  $P_i$  with multiplier function  $\text{mul}_i$ , and let  $M_i = M(P_i; \alpha_i; \text{mul}_i)$ . For  $i \in \{1, 2\}$  let  $L_i$  be the link corresponding to  $M_i$  as in Theorem 4.3. For  $i \in \{1, 2\}$ , let  $C_i$  be an edge component of  $L_i$  and let  $e_i$  be an edge of  $P_i$  which lies in the  $\alpha_i$ -edge cycle corresponding to  $C_i$ . We assume that either  $e_1$  has distinct vertices or  $e_2$  has distinct vertices. Let  $P_i^0$  be the faceted 3-ball obtained from  $P_i$  by replacing  $e_i$  with a digon  $D_i$  for  $i \in \{1, 2\}$ . See Figure 12. Because either  $e_1$  has distinct vertices or  $e_2$  has distinct vertices, we obtain a faceted 3-ball  $P$  from  $P_1^0$  and  $P_2^0$  by cellularly identifying  $D_1$  and  $D_2$ . We refer to  $P$  as a connected sum of  $P_1$  and  $P_2$  along  $e_1$  and  $e_2$ . The face-pairings  $\alpha_1$  and  $\alpha_2$  induce a face-pairing on  $P$ . Except for choices to be made involving corridors along either  $e_1$  or  $e_2$ , the corridor constructions for  $(P_1; \alpha_1)$  and  $(P_2; \alpha_2)$  which give rise to  $L_1$  and  $L_2$  induce a corridor construction for  $(P; \alpha)$ , which gives rise to an unframed link  $L$ . The isotopy type of  $L$  is uniquely determined by  $L_1, L_2$  and the identification of  $D_1$  and  $D_2$ . It is easy to see that  $L$  is a connected sum of  $L_1$  and  $L_2$  which joins  $C_1$  and  $C_2$ . We summarize this paragraph in the following theorem.

Figure 12. Replacing  $e_i$  with a digon  $D_i$ .Figure 13. The faceted 3-ball  $P$  and edge cycle multipliers.

**Theorem 5.2.1.** Let  $P_1$  and  $P_2$  be faceted 3-balls with orientation-reversing face-pairings  $\gamma_1$  and  $\gamma_2$ . Let  $L_1$  and  $L_2$  be corresponding unframed corridor complex links. Let  $C_1$  be an edge component of  $L_1$ , and let  $C_2$  be an edge component of  $L_2$ . Let  $e_1$  be an edge of  $P_1$  which lies in the  $\gamma_1$ -edge cycle corresponding to  $C_1$ , and let  $e_2$  be an edge of  $P_2$  which lies in the  $\gamma_2$ -edge cycle corresponding to  $C_2$ . Suppose that either  $e_1$  has distinct vertices or  $e_2$  has distinct vertices. Let  $P$  be a connected sum of  $P_1$  and  $P_2$  along  $e_1$  and  $e_2$ , and let  $L$  be the corresponding connected sum of  $L_1$  and  $L_2$  which joins  $C_1$  and  $C_2$ . Then  $L$  is an unframed corridor complex link associated to the orientation-reversing face-pairing on  $P$  induced by  $\gamma_1$  and  $\gamma_2$ .

*Proof.* This is clear from the previous paragraph.

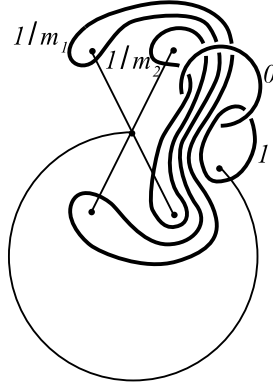
Suppose  $P_1$  and  $P_2$  are faceted 3-balls. For  $i \in \{1, 2\}$  let  $\gamma_i$  be an orientation-reversing face-pairing on  $P_i$  and let  $\text{mul}_i$  be a multiplier function for  $\gamma_i$ . Let  $e_1$  be an edge in  $P_1$  and let  $e_2$  be an edge in  $P_2$  such that  $\text{mul}_1([e_1]) = \text{mul}_2([e_2])$ . Then the multiplier functions  $\text{mul}_1$  and  $\text{mul}_2$  induce a multiplier function for the face-pairing induced by  $\gamma_1$  and  $\gamma_2$  on the connected sum of  $P_1$  and  $P_2$  along  $e_1$  and  $e_2$ .

### 5.3. Connected sums of bitwist manifolds.

**Theorem 5.3.1.** The connected sum of two bitwist manifolds is a bitwist manifold.

*Proof.* Let  $P$  be the faceted 3-ball with just two faces which are degenerate pentagons as in Figure 13. Let  $\gamma$  be the face-pairing on  $P$  which crosses the edge common to the two faces, and let  $\text{mul}$  be the multiplier function for  $\gamma$  indicated in Figure 13. Figure 14 shows a corridor complex and a corridor complex framed link  $L$  for  $\gamma$  and  $\text{mul}$ .

Now let  $P_1$  and  $P_2$  be faceted 3-balls with face-pairings and multiplier functions which give rise to bitwist manifolds  $M_1$  and  $M_2$ . We choose one of the two edges

Figure 14. The framed corridor complex link  $L$ .

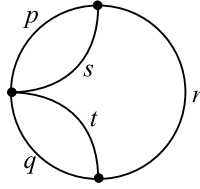
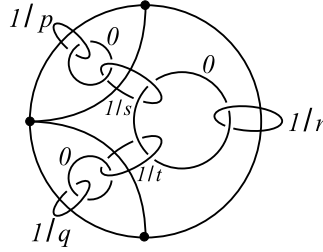
of  $P$  in the  $i$ -edge cycle with multiplier  $m_1$ , and we form a connected sum  $P_1^0$  of  $P$  and  $P_1$  along this edge and any edge of  $P_1$ . Next we choose one of the two edges of  $P$  in the  $j$ -edge cycle with multiplier  $m_2$ . This edge corresponds to an edge of  $P_1^0$ . We form a connected sum  $P_2^0$  of  $P_1^0$  and  $P_2$  along this edge and any edge of  $P_2$ . Theorem 5.2.1 easily implies that we obtain a twisted face-pairing manifold  $M$  which is the connected sum of  $M_1$ ,  $M_2$ , and a manifold which is obtained by Dehn surgery on a framed link which consists of two simply linked unknots with framings 0 and 1. This third connected summand is the 3-sphere. Thus  $M$  is the connected sum of  $M_1$  and  $M_2$ .

This proves Theorem 5.3.1.

**5.4. Reflection face-pairings.** We next consider face-pairings of a very special sort. We assume that our model faceted 3-ball  $P$  can be identified with the closed unit ball in  $\mathbb{R}^3$  so that the following holds. The intersection of the unit sphere with the  $xy$ -plane is a union of edges of  $P$  and the model face-pairing on  $P$  is given by reflection in the  $xy$ -plane. In other words, we have cell structures on both the northern and southern hemispheres of the unit sphere in  $\mathbb{R}^3$ , and the face-pairing maps of the model face-pairing are given by the map  $(x; y; z) \mapsto (x; y; -z)$ , which is therefore a cellular automorphism of  $P$ . In this case we call  $P$  a reflection faceted 3-ball, and we call a reflection face-pairing. Using the identification of  $P$  with the closed unit ball in  $\mathbb{R}^3$ , we speak of the equator of  $P$  and the northern and southern hemispheres of  $P$ .

Let  $P$  be a reflection faceted 3-ball with reflection face-pairing and multiplier function  $\text{mul}$ . As in Figure 15, we can describe  $P$ ,  $\sigma$ , and  $\text{mul}$  using a diagram which consists of a cellular decomposition of a closed disk together with a nonzero integer for every edge. We view this closed disk as the northern hemisphere of  $P$ . Hence we have the cellular decomposition of the northern hemisphere of  $P$ , which therefore determines the cellular decomposition of the southern hemisphere of  $P$ , and the integer attached to the edge  $e$  is  $\text{mul}(e)$ . We sometimes allow ourselves the liberty of attaching 0 to an edge instead of a nonzero integer. Attaching 0 to an edge means that every edge in the corresponding  $i$ -edge cycle collapses to a vertex.



Figure 15. The diagram corresponding to  $P$ ,  $\sigma$ , and  $\text{mul}$ .Figure 16. The framed link  $L$ .

Let  $P$  be a reflection faceted 3-ball with reflection face-pairing  $\sigma$ . Suppose given a multiplier function  $\text{mul}$  for  $\sigma$ , and let  $M$  be the associated bitwist manifold. Theorem 4.3 describes a framed link in the 3-sphere  $S^3$  such that Dehn surgery on this framed link gives  $M$ . In this paragraph we describe another framed link  $L$  in  $S^3$  such that Dehn surgery on  $L$  also gives  $M$ . We construct  $L$  as follows. We identify  $P$  with the closed unit ball in  $\mathbb{R}^3$  as in the definition of reflection faceted 3-ball. For every edge  $e$  of the northern hemisphere of  $P$  we choose an open topological ball  $B_e \subset \mathbb{R}^3$  such that  $B_e \setminus \partial P$  is a topological disk which meets  $e$  and is disjoint from every edge of  $P$  other than  $e$ . We assume that such topological balls corresponding to distinct edges are disjoint. For every face  $f$  of the northern hemisphere of  $P$  we construct an unknot  $C_f$  in the interior of  $f$  such that if  $e$  is an edge of  $f$ , then  $C_f$  meets  $B_e$ . These unknots are all components of  $L$  with framings 0. We call these components of  $L$  face components. Let  $2 \leq f \leq g$ . Every edge  $e$  of  $P$  in the northern hemisphere also gives a component  $C_e$  of  $L$ , called an edge component, as follows. Let  $e$  be an edge in the equator of  $P$  contained in the face  $f$  of the northern hemisphere. The  $\sigma$ -edge cycle of  $e$  is just  $feg$ . We define  $C_e$  to be a meridian of  $C_f$  contained in  $B_e$  with framing  $-\text{mul}(feg)$ . Now let  $e$  be an edge of the northern hemisphere of  $P$  not contained in the equator. Let  $f$  and  $g$  be the faces of  $P$  which contain  $e$ . Let  $x$  be a point of  $f \setminus B_e$  separated by  $C_f$  from  $\partial f$ , and let  $y \notin x$  be a point of  $g \setminus B_e$  separated by  $C_g$  from  $\partial g$ . The  $\sigma$ -edge cycle of  $e$  is  $E = fe;_f(e)g$ . We define  $C_e$  to be an unknot in  $B_e$  with framing  $-\text{mul}(E)$  such that  $P \setminus C_e$  is a properly embedded arc in  $P \setminus B_e$  joining  $x$  and  $y$ . This defines  $L$ .

Example 5.4.1. Let  $P$  be the reflection faceted 3-ball with reflection face-pairing  $\sigma$ , and multiplier function given by the diagram in Figure 15. Figure 16 shows the framed link  $L$  constructed above from these data using  $\text{mul} = 1$ .

Theorem 5.4.2. Let  $P$  be a reflection faceted 3-ball with reflection face-pairing  $\sigma$ . Suppose given a multiplier function for  $\sigma$ , and let  $M$  be the associated bitwist

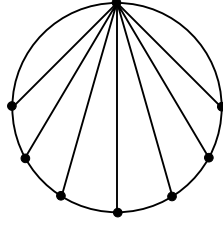


Figure 17. Top view of a scallop.

manifold. Let  $L$  be the framed link in  $S^3$  constructed above. Then Dehn surgery on  $L$  gives  $M$ .

Proof. Since  $L$  is amphicheiral, multiplying all framings by  $-1$  does not change the resulting manifold. So we may assume that  $\epsilon = 1$ . We show how to adapt [3, Theorem 6.1.2] to the present situation.

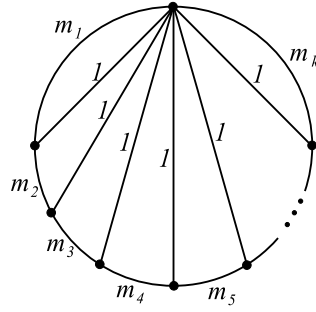
We construct a handlebody  $H$  as follows. We still identify  $P$  with the closed unit ball in  $\mathbb{R}^3$ . Let  $B$  be the topological ball which is the closure in  $S^3$  of  $S^3 \setminus P$ . We construct  $H$  by attaching handles to  $B$  as follows. Let  $f$  and  $f^{-1}$  be faces of  $P$  paired by  $\sigma$ . Then  $f$  and  $f^{-1}$  are joined by a vertical circular cylinder. We attach such a cylinder to  $B$ . Doing this for every pair of faces of  $P$  yields our handlebody  $H$ . It is clear that the closure in  $S^3$  of  $S^3 \setminus H$  is also a handlebody. We identify the components of  $L$  with curves in  $\partial H$  in a straightforward way.

As in [3, Theorem 6.1.2], let  $S$  be the edge pairing surface for the bitwisted face-pairing  $\sigma$ , let  $\gamma_1, \dots, \gamma_n$  be the vertical meridian curves of  $S$  and let  $\gamma_1, \dots, \gamma_m$  be core curves for the edge cycle cylinders. Then there exists a homeomorphism  $\phi : S \rightarrow \partial H$  such that  $\phi(\gamma_i)$  is the face component of  $L$  corresponding to  $\gamma_i$ , this face component being a meridian of  $H$ , for every  $i \in \{1, \dots, n\}$ . We also have that the edge components of  $L$  are parallel copies of  $\phi(\gamma_1), \dots, \phi(\gamma_m)$ . The framing determined by  $\partial H$  of every edge component of  $L$  is 0. Just as in the proof of Theorem 4.3, the statement and proof of [3, Theorem 6.1.2] go through in this greater generality. So Dehn surgery on  $L$  gives  $M$ .

5.5. Lens spaces. In this subsection we show that every lens space is a twisted face-pairing manifold. We will use this in the proof of Theorem 5.6.1.

We begin by defining the notion of a scallop. A scallop is a reflection faceted 3-ball  $P$  (defined in Section 5.4) whose northern hemisphere has a cell structure essentially as indicated in Figure 17. More precisely, every vertex of a scallop  $P$  lies on the equator of  $P$ ,  $P$  contains a vertex  $v$  such that every edge of  $P$  not contained in the equator of  $P$  joins  $v$  with another vertex, and every vertex of  $P$  other than  $v$  is joined with  $v$  by at least one edge. So the northern hemisphere of a scallop might consist of just a monogon. Otherwise it is subdivided into digons and triangles, in which case it has at least two digons, but it may have arbitrarily many digons.

Theorem 5.5.1. Let  $P$  be a scallop with  $k$  faces in its northern hemisphere. Let  $\sigma$  be a reflection face-pairing on  $P$ , let  $\text{mul}$  be a multiplier function for  $\sigma$ , and let  $M = M(P; \sigma; \text{mul})$ . Suppose that  $P$ ,  $\sigma$ , and  $\text{mul}$  are given by the diagram in Figure 18, where  $m_1 > 0$ ,  $m_k > 0$ , and  $m_i = 0$  for  $i \in \{2, \dots, k-1\}$ . (If a multiplier is 0, then the corresponding edge in Figure 18 collapses to a vertex of


 Figure 18. The diagram for  $P$ , and  $\text{mul}$ .

$P$ .) Define integers  $a_1, \dots, a_k$  so that  $a_1 = m_1$  if  $k = 1$  and if  $k > 1$ , then  $a_1 = m_1 + 1$ ,  $a_k = m_k + 1$ , and  $a_i = m_i + 2$  for  $i = 2, \dots, k-1$ . Then there exist relatively prime positive integers  $p, q$  such that  $M$  is homeomorphic to the lens space  $L(p; q)$ , where

$$\frac{p}{q} = [a_1; a_2; a_3; \dots; (-1)^{k+1} a_k] = a_1 + \cfrac{1}{a_2 + \cfrac{1}{a_3 + \cfrac{1}{\ddots + \cfrac{1}{a_{k-1} + \cfrac{1}{a_k}}}}}$$

(It is possible that  $p = q = 1$ , in which case we obtain the 3-sphere.) Furthermore, given relatively prime positive integers  $p$  and  $q$  with  $p \neq q$ , then there exists a unique sequence of integers  $m_1, \dots, m_k$  as above such that the above continued fraction equals  $p/q$ .

*Proof.* Theorem 5.4.2 implies that  $M$  is given by Dehn surgery on the framed link in Figure 19, where for convenience we have chosen  $\text{framing} = 1$ . We repeat that if  $m_i = 0$  for some  $i = 2, \dots, k-1$ , then the corresponding edge in Figure 18 collapses to a vertex of  $P$ . In this case the corresponding component of the link in Figure 19 is to be removed. This is consistent with the fact that any component with framing 1 may be removed from a framed link without changing the resulting manifold. We next use Kirby calculus to simplify the framed link in Figure 19. For every  $i = 1, \dots, k$  we perform the slam-dunk which removes the component with framing  $1 = m_i$ . In doing this, the component linked with the given component acquires the framing  $m_i$ . We next perform a Rolfsen twist about every component shown in Figure 19 with framing 1. Every such component is then removed, and 1 is added to the framing of the components linked with it. The resulting framed link is shown in Figure 20. It follows from page 272 of [8] or page 108 of [7] or just by iterating slam-dunks that  $M$  is the lens space as stated in Theorem 5.5.1.

The uniqueness statement is well known. For this, first note that if  $k = 1$ , then  $a_1$  is an arbitrary positive integer. If  $k > 1$ , then  $a_1, \dots, a_k$  are arbitrary integers with  $a_i \geq 2$  for  $i = 1, \dots, k$ . Given  $p$  and  $q$ , we calculate  $a_1, \dots, a_k$  by modifying the division algorithm usually used to calculate continued fractions. Instead of taking the greatest integer less than or equal to our given number, we take the

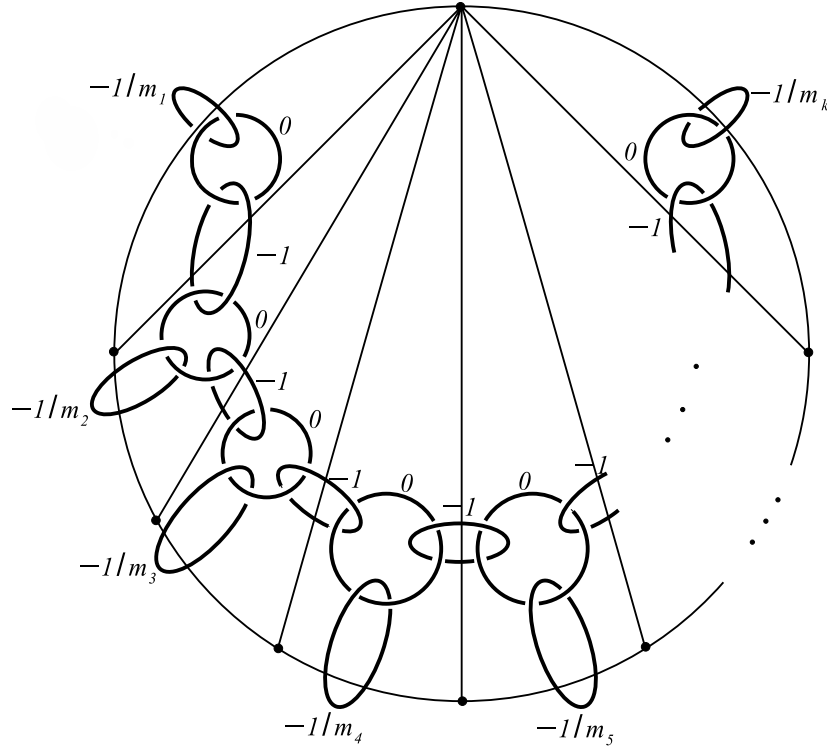
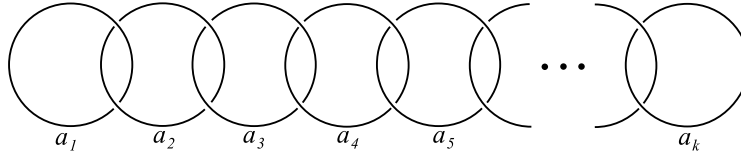


Figure 19. The framed link corresponding to Figure 18.

Figure 20. Dehn surgery on this framed link gives  $M$ .

least integer greater than or equal to our given number. The details are left to the reader.

This proves Theorem 5.5.1.

Corollary 5.5.2. Every lens space is a twisted face-pairing manifold.

5.6. Changing the framings. Suppose given an orientation-reversing face pairing on a faceted 3-ball  $P$ . In Section 4 we construct a corridor complex link  $L$  by means of link projections. The face components of  $L$  correspond to the face-pairs of  $P$ , and the edge components of  $L$  correspond to the edge cycles of  $P$ . Given the extra information of a multiplier function  $m$ , we define framings on the components of  $L$ . We define the framing of each face component to be 0. If  $C$  is an edge component, then we define the framing of  $C$  to be the blackboard framing of  $C$  plus  $m(E)^1$ , where  $E$  is the edge cycle corresponding to  $C$ . By Theorem 4.3, performing Dehn



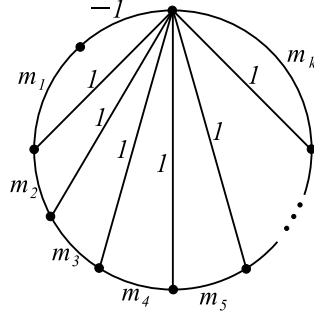


Figure 22. The reflection faceted 3-ball  $P_i$  when  $i \geq N$  and  $\epsilon_i > 0$ .

edge in  $P_i$  which is immediately to the left of the top vertex in Figure 21 or 22. Since the multipliers are compatible on edge cycles that are amalgamated, they define a multiplier function for  $\mathcal{P}^0$ .

We next construct a framed corridor complex link for  $(\mathcal{P}^0; \mathcal{P}^0)$ . If  $i \geq N$  and  $\epsilon_i = 0$ , then the link  $K_i$  shown in Figure 23 is a framed link for  $(P_i; \epsilon_i)$  as in Figure 19. This framed link is in fact isotopic to a framed corridor complex link for  $(P_i; \epsilon_i)$ . If  $i \geq N$  and  $\epsilon_i > 0$ , then one gets a framed corridor complex link  $K_i$  from the link in Figure 23 by multiplying the framing of each component by  $-1$ . By repeated applications of Theorem 5.2.1, one gets a framed corridor complex link  $J$  for  $(\mathcal{P}^0; \mathcal{P}^0)$ .

Suppose  $i \geq N$  and  $\epsilon_i = 0$ . Figure 24 shows part of  $J$  corresponding to  $K_i$ . As in the proof of Theorem 5.5.1, we can simplify this to obtain the framed link in Figure 25. A gain as in the proof of Theorem 5.5.1, by performing  $k-1$  slam-dunks, we may reduce  $J$  to the framed link in Figure 26. A similar argument holds if  $i \geq N$  and  $\epsilon_i > 0$ , except that the framing of the meridian component is  $r_i$  instead of  $\epsilon_i$ .

Finally, one performs a slam dunk for each  $i \geq N$ . If  $\epsilon_i = 0$ , then the framing of  $C_i$  becomes

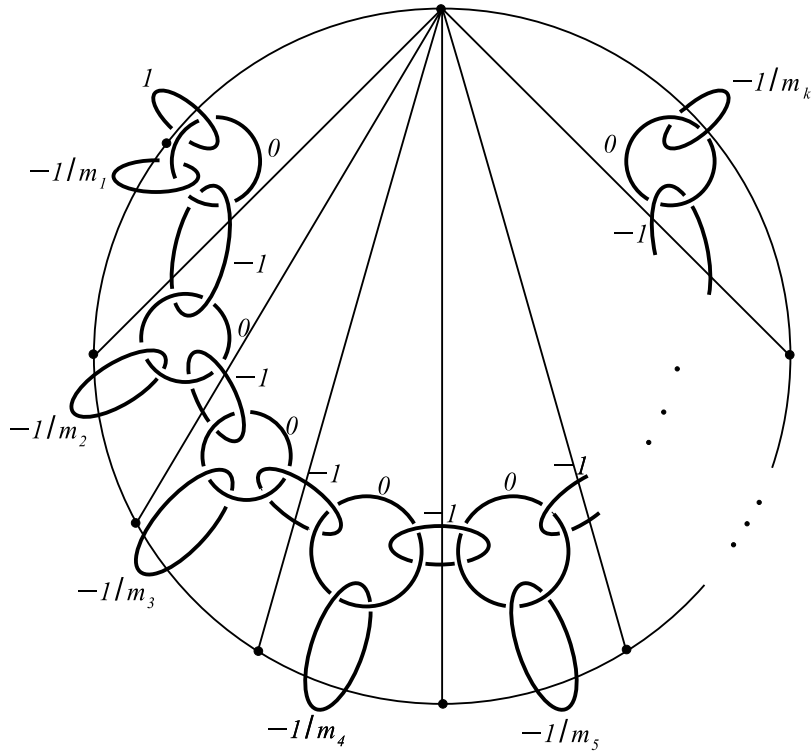
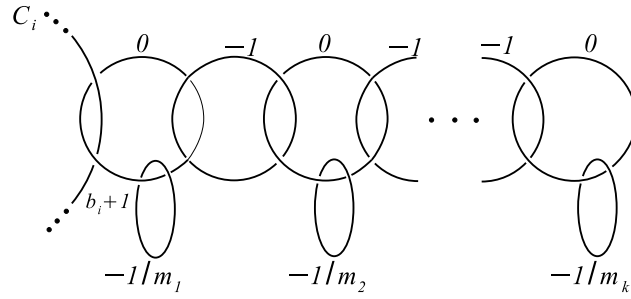
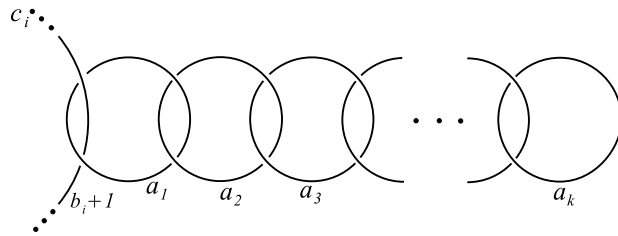
$$b_i + \text{mul}(E_i) - \frac{1}{r_i} = b_i + 1 \quad (1 - \epsilon_i) = b_i + \epsilon_i:$$

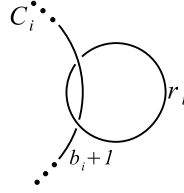
If  $\epsilon_i > 0$ , then we have  $b_i - 1 + (1 + \epsilon_i) = b_i + \epsilon_i$ . So Dehn surgery on the framed link  $L$  is a bitwist manifold.

## 6. Realizing 3-manifolds as bitwist manifolds

In this section we show that every closed connected orientable 3-manifold is a bitwist manifold.

Let  $B$  be a braid with  $n$  strands. Following [7], we consider the strands of  $B$  as joining the points  $A_i = (i; 0; 0)$  and  $B_i = (i; 0; 1)$  in  $\mathbb{R}^3$ ,  $1 \leq i \leq n$ . The closure of  $B$  is a link in  $S^3 = \mathbb{R}^3 \cup \{\infty\}$  obtained by joining each  $A_i$  and  $B_i$  by an arc such that the projections of these arcs on the  $xz$ -plane are disjoint from each other and from the projection of  $B$  onto the  $xz$ -plane. By a generalized closure, we only assume that the endpoints  $fA_i: 1 \leq i \leq n$  and  $fB_i: 1 \leq i \leq n$  are joined by  $n$  arcs whose projections are disjoint from each other and from the projection of  $B$ . This


 Figure 23. The framed link  $K_i$  when  $i = 0$ .

 Figure 24. Part of the framed link  $J$ .

 Figure 25. Simplifying the framed link  $J$ .

Figure 26. Simplifying the framed link  $J$ .

agrees with the definition of closure given in §1, but is more restrictive than that because we are not allowing any more crossings in the projection.

**Lemma 6.1.** Every link  $L$  is a generalized closure of a pure braid.

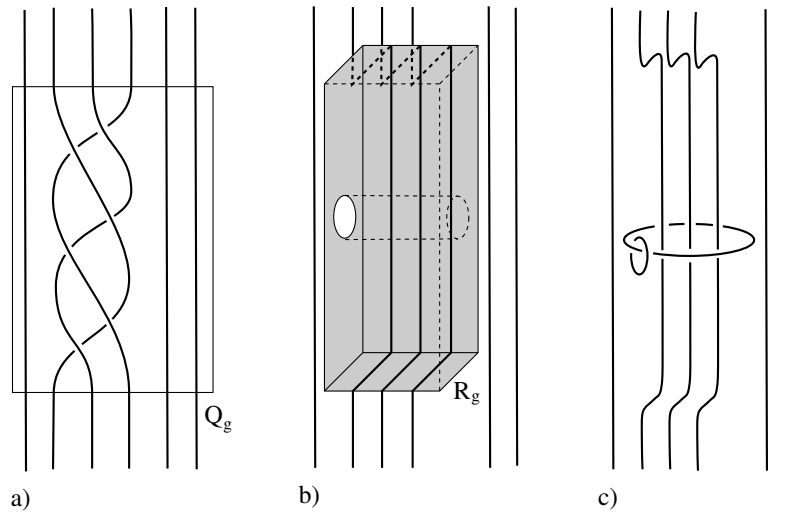
**Proof.** Let  $L$  be a link in  $\mathbb{R}^3$ , and let  $\pi : \mathbb{R}^3 \rightarrow \mathbb{R}$  be the projection onto the third coordinate. Then  $L$  can be isotoped so that, for some integer  $n$ , the height function on  $L$  has  $n$  local maxima, which lie in  $\pi^{-1}((1; 1))$  and  $n$  local minima, which lie in  $\pi^{-1}((-1; 0))$ . Furthermore, we can assume that  $L$  intersects the  $xy$ -plane in the points  $A_i = (i; 0; 0)$ ,  $1 \leq i \leq 2n$ ,  $L$  intersects the plane  $z = 1$  in the points  $B_i = (i; 0; 1)$ ,  $1 \leq i \leq 2n$ , and all crossings of the projection of  $L$  onto the  $xz$ -plane lie in  $\pi^{-1}([0; 1])$ . (This follows, for example, from Alexander's theorem, which states that  $L$  can be represented as the closure of an  $n$ -strand braid.) For convenience, we call the components of  $L \setminus \pi^{-1}([0; 1])$  the strands of  $L$ , we call the components of  $L \setminus \pi^{-1}([1; 1))$  the tops of  $L$ , and we call the components of  $L \setminus \pi^{-1}((-1; 0])$  the bottoms of  $L$ . We first isotope  $L$  to a link  $L_1$  so that there is a strand of  $L_1$  joining  $A_1$  and  $B_1$  and so that there is a top of  $L_1$  joining  $B_1$  and  $B_2$ . This can be done by sliding tops past each other and possibly introducing a crossing in the projection of one top to change the order of its endpoints in the projection. If the strand of  $L_1$  descending from  $B_2$  ends at  $A_2$ , then we repeat this process starting with the strand rising from  $A_3$ . Otherwise, by sliding bottoms of  $L_1$  past each other and possibly adding a crossing in the projection of one bottom of  $L_1$ , we can isotope  $L_1$  to a link  $L_2$  such that there is a strand of  $L_2$  joining  $A_1$  and  $B_1$ , there is a top of  $L_2$  joining  $B_1$  and  $B_2$ , there is a strand of  $L_2$  joining  $B_2$  and  $A_2$ , and there is a bottom of  $L_2$  joining  $A_2$  and  $A_3$ . One next considers the strand rising from  $A_3$ . One can continue this process to isotope  $L$  to a generalized closure of a pure braid with  $2n$  strands.

We next consider generators for the pure braid group. Let  $K_n$  be the pure braid group of isotopy classes of  $n$ -stranded pure braids. Given  $1 \leq i < j \leq n$ , let  $b_{i,j}$  be the pure braid obtained by doing a full twist on the collection of strands from the  $i^{\text{th}}$  to the  $j^{\text{th}}$ . Then (if the directions of twisting are chosen properly)  $a_{i,j} = b_{i,j} b_{i+1,j}^{-1}$  is a pure braid for which the  $i^{\text{th}}$  strand goes in front of the  $k^{\text{th}}$  strands,  $i < k \leq j$ , and then behind the  $k^{\text{th}}$  strands,  $i < k \leq j$ . Since the elements  $a_{i,j}$ ,  $1 \leq i < j \leq n$ , generate the pure braid group, the elements  $b_{i,j}$ ,  $1 \leq i < j \leq n$ , generate the pure braid group.

**Theorem 6.2.** Every closed connected orientable 3-manifold is a bitwist 3-manifold.

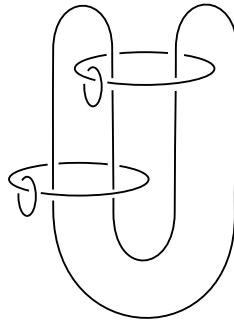
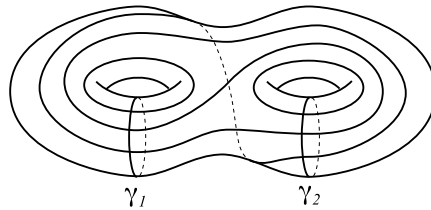
**Proof.** Suppose  $M$  is a closed connected orientable 3-manifold. By the Dehn-Lickorish theorem,  $M$  can be obtained by Dehn surgery on a framed link  $L$ . By




 Figure 27. Steps in the construction of  $L^0$ .

Theorem 5.3.1 we can assume that  $L$  is not a split link. By Lemma 6.1,  $L$  is a generalized closure of a pure braid  $B$ . We write  $B$  in terms of the generators  $b_{i,j}$ . We now view our projection of  $L$  as lying in the plane  $\mathbb{R}^2$ . We view the braid  $B$  as lying in a rectangle  $R$ , with its strands joining the top and the bottom. The generators of  $B$  lie in subrectangles which stack together to give the rectangle  $R$ . Choose such a subrectangle  $Q_g$  corresponding to a generator  $g$  of  $B$ . See Figure 27 a). Then  $g$  is a full twist on a set of consecutive strands of the braid in  $Q_g$ . Let  $R_g$  be a subrectangle of  $Q_g$  which contains only the consecutive strands that are twisted in  $g$ . We next attach a rectangular block to  $R$  so that the bottom of the block is on  $R_g$ . The side of the block facing the top of  $R$  is the front of the block, and the side of the block facing the bottom of  $R$  is the back of the block. We replace the strands of  $R_g$  that are twisted by parallel strands that go over the front of the block, along the top of the block, and then back down the back of the block. We also drill out a hole in the block that goes through the sides. See Figure 27 b). In effect, we have added a handle to the surface, and have replaced  $g$  by a trivial braid which goes over the handle. We also choose a circle for the boundary of the block's hole, and we choose a meridian for the handle. We expand the meridian slightly so that it links the arcs that go over the handle and the circle in the boundary of the hole. See Figure 27 c). We choose framing 0 for the meridian, and framing  $-1$  (depending on the direction of twist of the generator) for the circle in the boundary of the hole. We shrink the block slightly so that blocks corresponding to different subrectangles are disjoint. Doing this for each generator while maintaining the framings of the components of  $L$  gives a framed link  $L^0$ . Let  $S$  be the surface obtained from the 2-sphere  $\mathbb{R}^2 \cup \{\infty\}$  by adding a handle as described above for each generator of  $B$ .

If we perform a slam-dunk on each circle along the boundary of a hole, then the effect on  $L^0$  is to delete those circles and to change the framing on each of the meridian circles to  $-1$ . If we now perform a Rolfsen twist along each of the meridian circles, then we recover the original link  $L$ , but with framings changed by sums and differences of squares of linking numbers of the meridian curves and the components

Figure 28. The link  $L^0$  for a simple example.Figure 29. The surface  $S$  with meridians and nonmeridian link components.

of  $L$ . Hence if we change the framings on  $L^0$  by adding an appropriate integer to each of the components of  $L$ , we get a framed link  $L^0$  such that  $M$  is obtained from the 3-sphere by surgery on  $L^0$ . By Theorem 5.6.1, to prove Theorem 6.2 it suffices to prove that  $L^0$  is a corridor complex link whose face components are the meridians.

To get a face pairing, we cut open the surface  $S$  along the meridians. If there are  $n$  meridians, the result is a 2-sphere with  $2n$  paired holes and disjoint arcs joining their boundaries. We attach a disk to every hole to obtain a 2-sphere  $S^0$ . Since  $L$  is not a split link, the connected components of the complement in  $S^0$  of the union of the arcs and closed disks are all simply connected. The link in Figure 28 gives rise to the surface with curves in Figure 29 (which is taken from [3]). Figure 30 shows the result  $S^0$  of cutting open  $S$  and attaching disks. We fatten each arc to a quadrilateral, foliated by arcs parallel to the core arc, so that adjacent quadrilaterals touch on the boundaries of the  $2n$  disks. See, for example, Figure 31. We now collapse to a point each leaf in a quadrilateral and the closure of each region in the complement of the union of the paired disks and foliated quadrilaterals. By Moore's theorem the quotient space  $S^0$  is a 2-sphere, with a cell structure that consists of a vertex for each collapsed complementary region, an edge for each collapsed foliated quadrilateral, and a face for each of the  $2n$  paired disks. We define a face-pairing on the quotient space  $S^0$  in a straightforward way. This defines a face-pairing for a faceted 3-ball  $P$  whose boundary is the 2-sphere  $S^0$ . For the example above, this is shown in Figure 32. By construction,  $L^0$  is a corridor complex link for  $(P; \cdot)$ .

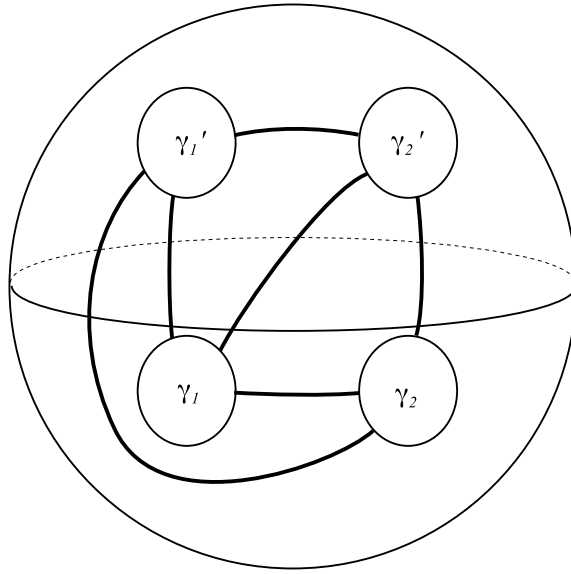


Figure 30. Cutting open the surface  $S$  to get  $S^0$ .

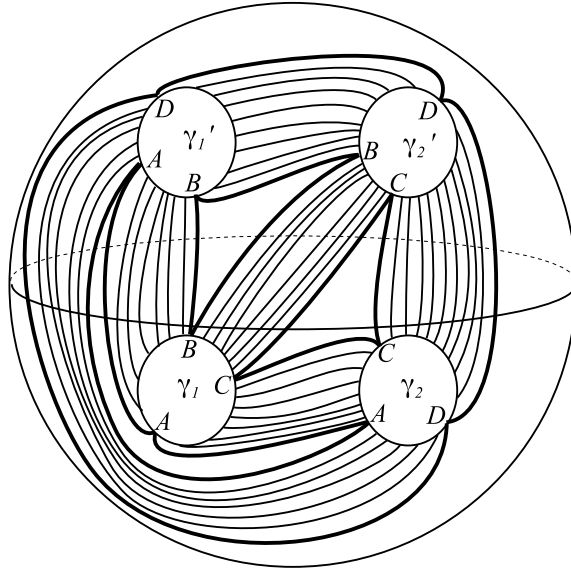


Figure 31. Constructing the faceted 3-ball.

### References

- [1] J.W .Cannon, W .J.Floyd, and W .R .Parry, Introduction to twisted face-pairings, M ath . Res. Lett. 7 (2000), 477{491.
- [2] J.W .Cannon, W .J.Floyd, and W .R .Parry, Twisted face-pairing 3-m anifolds, Trans. Am er. M ath. Soc. 354 (2002), 2369{2397.
- [3] J.W .Cannon, W .J.Floyd, and W .R .Parry, Heegaard diagram s and surgery descriptions for twisted face-pairing 3-m anifolds, A lgebr. G eom . Topol. 3 (2003), 234{285 (electronic).

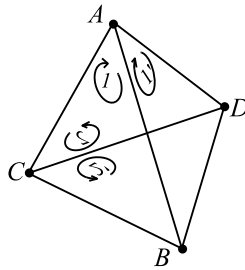


Figure 32. The face-pairing on the faceted 3-ball.

- [4] N.M. Dunfield and W.P. Thurston, Finite covers of random 3-manifolds, *Invent. Math.* 166 (2006), 457{521.
- [5] R.E. Gompf and A.I. Stipsicz, 4-Manifolds and Kirby Calculus, Graduate Studies in Math., Vol. 20, Amer. Math. Soc., Providence, 1999.
- [6] A. Kawachi, A Survey of Knot Theory, Birkhauser Verlag, Basel-Boston-Berlin, 1996.
- [7] V.V. Prasolov and A.B. Sossinsky, Knots, Links, Braids and 3-Manifolds, Amer. Math. Soc., Providence, 1997.
- [8] D. Rolfsen, Knots and Links, Math. Lecture Series 7, Publish or Perish, Wilmington, 1976.

Department of Mathematics, Brigham Young University, Provo, UT 84602, U.S.A.  
 E-mail address: cannon@math.byu.edu

Department of Mathematics, Virginia Tech, Blacksburg, VA 24061, U.S.A.  
 E-mail address: floyd@math.vt.edu  
 URL: <http://www.math.vt.edu/people/floyd>

Department of Mathematics, Eastern Michigan University, Ypsilanti, MI 48197, U.S.A.  
 E-mail address: walter.parry@emich.edu